Graphical Abstract

Non-invasive Temperature Measurement in Fixed Bed Reactors using RFID Technology

Steffen Flaischlen, Gregor D. Wehinger

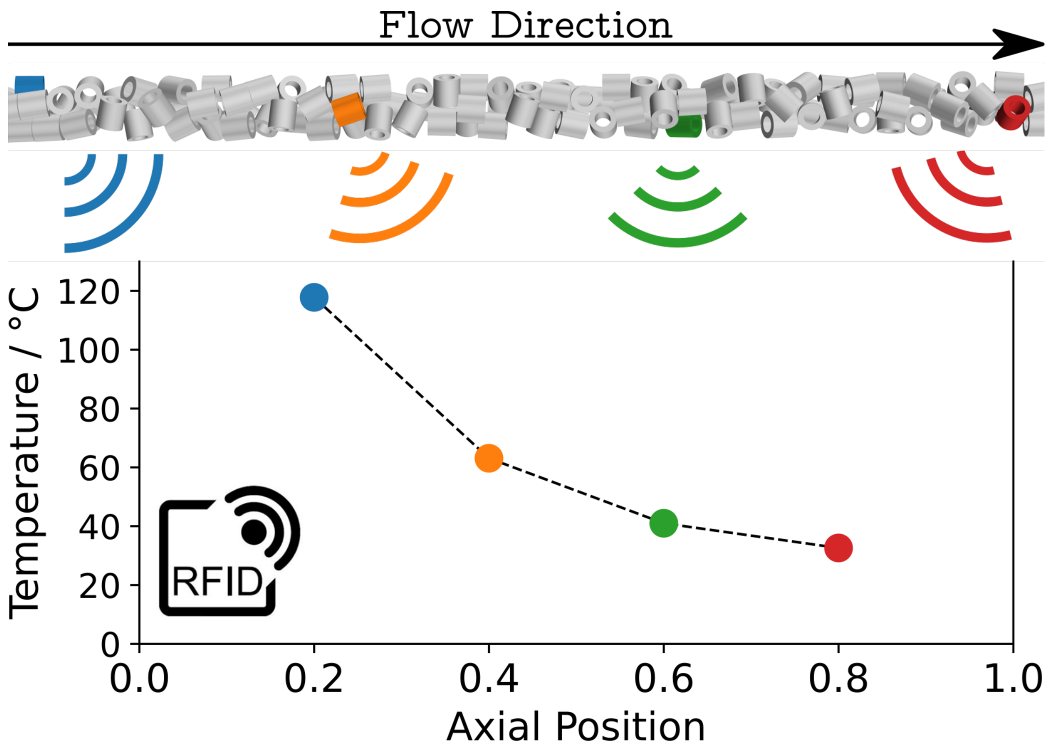

Highlights

Non-invasive Temperature Measurement in Fixed Bed Reactors using RFID Technology

Steffen Flaischlen, Gregor D. Wehinger

- Using radio frequency identification (RFID) for contactless temperature measurement
- RFID tags measure non-invasive temperature ($20 < T < 140$ °C) inside packed beds.
- RFID tags can be integrated in 3D printed pellets to avoid bed structure changes.
- Response time of RFID technology is similar to conventional thermocouples.
- Recent constraints of RFID tags show needs for further improvements.

Non-invasive Temperature Measurement in Fixed Bed Reactors using RFID Technology

Steffen Flaischlen[a,b], Gregor D. Wehinger[a,b,c,*]

[a] *Clausthal University of Technology, Institute of Chemical and Electrochemical Process Engineering, Leibnizstraße 17, 38678 Clausthal-Zellerfeld, Germany*
[b] *Clausthal University of Technology, Research Center Energy Storage Technologies (EST), Am Stollen 19A, 38640 Goslar, Germany*
[c] *Karlsruhe Institute of Technology, Institute of Chemical Process Engineering, Fritz-Haber-Weg 2, 76131 Karlsruhe, Germany*

Abstract

Measuring axial temperature profiles in fixed bed reactors is essential for an optimal and safe operation. Typically, thermocouples are used which influence the bed structure - especially in arrangements with a low ratio between tube and particle diameter - and thus local transport phenomena and reaction rates. In this publication, radio frequency identification (RFID) tags are used for temperature measurement in fixed beds without disturbing the bed structure. Therefore, the temperature is compared in a tubular fixed bed ($D = 25.4\,\mathrm{mm}$) of ceramic rings ($d_\mathrm{p} = 10\,\mathrm{mm}$) measured with RFID tags and thermocouples at similar axial positions at different temperature levels $20 < T < 140$ °C. By integrating an RFID tag into a particle using 3D printing, the disturbance of the fixed bed by the measurement device can be even completely avoided. It is shown that the overall values of temperature and the dynamic measurement with RFID tags is comparable to measurements using thermocouples. However, significant measurement gaps can occur, especially with unfavorable antenna-tag alignment or small antenna spacing. As a

*Corresponding author
Email address: gregor.wehinger@kit.edu (Gregor D. Wehinger)

summary, it is possible to measure temperature in fixed-bed reactors using RFID technology without requiring direct access and thus disturbing the bed structure. Finally, current shortcomings of RFID are discussed, and research needs presented.

Keywords: Temperature measurement, Fixed bed reactor, Process monitoring, RFID, 3D printing

1. Introduction

In various technical applications, such as trickle bed reactors, separation columns, pebble bed reactors, and fixed bed reactors, random packings consisting of defined particles are used [1, 2, 3, 4]. In chemical engineering, these particles, also known as pellets, are typically made of ceramics and are often designed to have specific properties, such as high surface area or good heat transfer capabilities. Using defined particles in chemical reactors help to optimize processes by improving mass and heat transfer [5], reducing pressure drop [6], and increasing reaction efficiency [7]. Since the reactor performance depends on the process variables, i.e., local concentration and temperature, their measurement is essential to achieve the optimum operating point. Especially in fixed bed reactors where chemical surface reactions occur, temperature plays a major role in influencing important quantities, such as conversion and selectivity, and to avoid catalyst deactivation, thermal degradation or reactor runaway. Typical temperature ranges in which fixed bed reactors are operated are between 200 and 1000 °C [8]. However, external cooling or heating is required to achieve the desired conversion and to prevent side reactions. This leads to a complex interplay between reaction enthalpy, heat transport within the fixed bed, and cooling temperature, which must be carefully controlled to maintain the reactor temperature within a precisely defined range [9]. Therefore, temperature measurement inside fixed bed reactors is essential for process monitoring and safety concerns.

Thoméo et al. have evaluated methods for measuring temperature distributions in packed beds [10]. For catalytic fixed beds, only techniques utilizing embedded thermowells or capillaries with moveable or multi-point thermocouples are appropriate. Thermocouples are either relocated radially through the reactor wall [11, 12, 13] or placed axially [14, 15]. A number of axially inserted thermocouples at various radial positions or, equivalently, a number of radial thermocouples installed at varying bed lengths would be necessary to monitor a three-dimensional temperature field. In any instance, heat conduction along the metal sheath of the temperature sensor causes the temperature profile itself to be altered in addition to the flow through the packing being affected [16].

In the case of multi-tubular reactors with many hundreds or thousands of tubes, this means that the measured temperature may no longer be representative of all other undisturbed tubes [17]. Recently, a couple of theoretical studies using Particle-resolved Computational Fluid Dynamics (CFD) quantified the influence of thermowells on heat transfer and reaction rates in slender packed beds [18, 19, 20]. These studies underpin that the invasive nature of common temperature measurement techniques in slender packed beds leads to uncertainties for process monitoring in multi-tubular reactors.

An alternative measurement technique to thermocouples are fiber optic systems which consist of thin fibers measuring temperature (and strain) with a high axial resolution. The two most common approaches are Fiber Bragg Grating (FBG) sensors and the Distributed Optical Fiber Sensing (DOFS) technology [21]. FBG is based on the variation of the refractive index, i.e., the Bragg grating, in the core of a waveguide and has measurement points applied at discrete positions (several millimeter to meter) on the fiber. This narrow reflection spectrum has a wavelength that responds to strain and temperature changes, allowing for simultaneous measurements of both quantities [22]. However, in the case of fixed beds, any change in strain must be minimized to accurately measure temperature only. FBG was applied successfully to measure temperature axially and radially in catalytic fixed bed reactors [23, 24]. In order to continuously monitor temperature, DOFS or distributed temperature sensing (DTS) systems can be used with a single optical fiber over distances of up to hundreds of meters [25]. In general, DTS operates under the principle of optical frequency domain reflectometry, which detects external disturbances using for example Rayleigh backscatter techniques. Recently, the dynamic cooling behavior in a nuclear reactor pebble bed was measured with DTS with a spacial resolution of 2.5 mm at 250 Hz [26]. For fixed bed reactors, the DTS system was used by Bremer [27] in order to measure a finely resolved axial temperature profile (approx. 1000 points per meter) of a two meter long industrial scale single tube fixed bed reactor. The author monitored the temperature evolution steady and dynamic experiments in order to validate a detailed reactor model. Despite their high dynamic measurements and axial resolution, fiber optic systems share the same limitation as thermocouples in that they interfere with the fixed bed structure due to their positioning. Other common temperature measurement techniques, such as pyrometers and thermal imagers, need optical accessibility to the bed interior or are placed in axial capillaries [28], too.

Since invasive methods have significant effects on the fixed bed structure, non-invasive methods should be preferred for temperature measurement in fixed bed reactors with small tube-to-particle-diameter ratios. In this regard, the use of temperature-sensitive paint (TSP) seems attractive [29]. TSP is coated on the surface of interest and then responds to changes in temperature with a change in color [30]. The immediate change of color makes reversible TSP suitable for monitoring in real-time, but it also requires optical accessibility to the surface. Therefore, TSP is typically applied on surfaces with external flow [31]. On the other hand, non-reversible temperature-sensitive paint may offer information on maximum values of a surface without requiring optical accessibility. This technique may be applied in fixed-bed reactors in the future. With a permanent color change, the maximum temperature on each pellet may be determined after the reactor is emptied pellet-wise.

The measurement methods presented thus far have limitations that render them imperfect for use in a fixed bed reactor. These limitations include their potential to influence the fixed bed structure and the requirement for optical accessibility. In the field of process engineering, there is already initial work on the use of contactless data transmission using Radio-Frequency Identification (RFID) technology, e.g., in thermal insulation, or in heating cables to monitor temperature [32, 33]. While this work focus on temperature measurement with RFID, there are other quantities that can be measured. Hillier et al. used a passive Ultra High-Frequency sensor to measure concentration in aqueous electrolyte solutions [34]. Eom et al. monitored the freshness of vegetables by oxygen and carbon dioxide concentration using a gas sensor in combination with an RFID tag [35]. The pressure in a bioprocess was measured by Surman et al. using a pressure-sensitive flexible membrane on an RFID transducer [36]. Ong et al. describe a platform for a passive RFID sensor that can measure complex quantities of a surrounding fluid, i.e., permittivity, temperature, humidity, and pressure [37].

In this work, a temperature measurement method using RFID data transmission is introduced, which does not exert an influence on the structure of a fixed bed reactor. Consequently, a configuration featuring a small reactor-tube-to-particle diameter ratio was employed, as it is of particular interest due to the resulting localized structure within the fixed bed. Additionally, a small tube diameter was selected to replicate the characteristics of an individual tube within a tube bundle reactor configuration typically employed for highly exothermic or endothermic reactions [38, 39, 40, 41, 42]. RFID tags with 14 mm in diameter and 2 mm in height are used for this purpose. They transmit the temperature from inside the fixed bed reactor to the outside without direct contact. Compared to other measurement methods, it has the advantage that the reactor does not have to be optically accessible and online measurement is possible during operation. Temperature measured with the RFID tags is compared to conventional thermocouples in a fixed bed with a hot air stream under constant and dynamic heating. Furthermore, the possibility of 3D printing allows the RFID tags to be inserted directly into a pellet, which not only completely eliminates the influence on the fixed bed structure, but also may make completely new experimental data accessible. Finally, limitations of the current RFID tags are discussed and future research needs are presented.

2. Material and methods

2.1. Radio-Frequency Identification (RFID) Technology

Radio-Frequency Identification (RFID) is a technology for the contactless transmission of information over a short distance by using high-frequency radio waves [43]. The sensor network consists of transponders (tags) and interrogators (readers). Tags are attached to objects; and readers communicate with the tags in their specified transmission ranges via radio signals [44]. When the transponder is in range of the transmitter, it is triggered by the electromagnetic field and can send digital data to the receiver. The transponders can be divided into three classes, which have different characteristics. Active and semi-passive transponders have their own battery, which enables them to transmit signals over a longer range.

In contrast, passive sensors are powered inductively via the electromagnetic field, which limits their range compared to the other two types. However, they are also the cheapest and have the smallest dimensions due to the lack of a battery. Therefore, the choice of transponder depends on the specific application requirements, such as the desired range and cost. More detailed information on transponder classes, etc. can be found elsewhere [45, 46]. Another important factor is the frequency at which the system operates. This can also be differentiated into communication ranges, whereby the passive read distance also becomes larger with increasing frequency. However, higher frequencies also lead to limitations, as transponders operating in the ultra-high frequency (UHF) range (868 - 928 MHz) no longer transmit reliable signals when they are close to liquids or metals. Transponders in the high-frequency (HF) range (13.56 MHz), on the other hand, only have a limited communication distance of $10-20$ cm. The system used for this work operates in the HF range, since the fixed bed reactor is always in the vicinity of metal pipes or components due to the surrounding periphery. Furthermore, the use of liquid reactants in the reactor may be possible, as well as the heating of the outer wall with water or thermal oil. Such liquids typically also lead to a disturbance of the signal. This reduces the possible range for the system used, which should prevent interference.

The RFID tags used for temperature measurement operate on the principle of a semiconductor sensor based on the temperature and current characteristics of a transistor. The operation of identical transistors with different collector current densities can be used to determine the absolute temperature from the difference in their base-emitter voltages [47].

2.2. Experimental Setup

The experimental setup consists of a reader, several antennas, and RFID temperature-measuring transponder tags, all manufactured by Micro-Sensys GmBH (Erfurt, Germany) and operate in the HF range of 13.56 MHz. The reader generates an HF electromagnetic field for ensuring the power supply of the passive transponders. Since the position of the transponder tag in the fixed bed cannot be precisely determined during the filling process, a system containing round antennas is chosen. These can be positioned around the reactor so that the scanning takes place independently of the direction of the tags. This means that the transponder does not have to be aligned

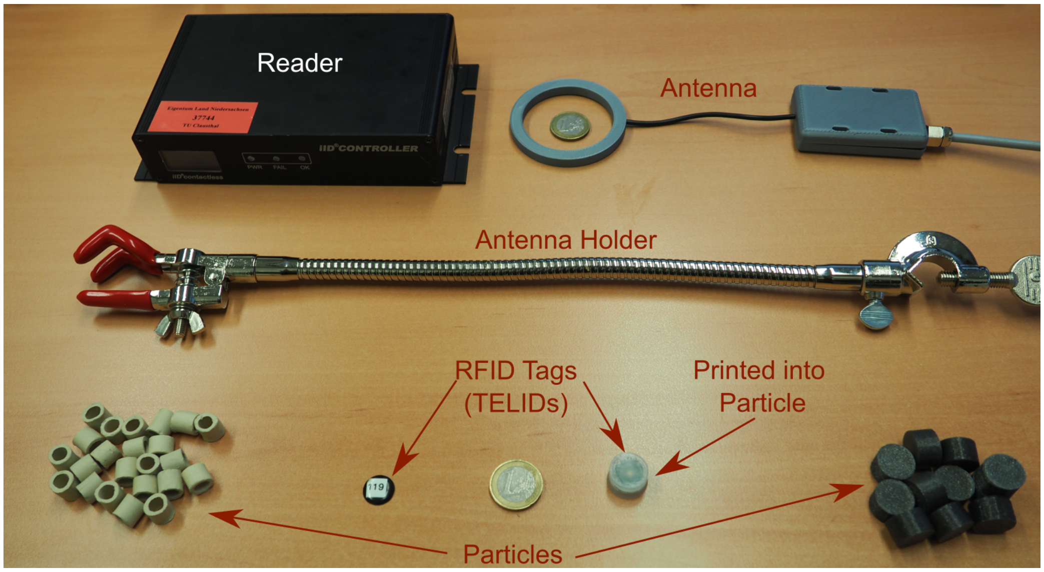

Figure 1: All parts of the measurement setup. Note that the 1 € coin has an outer diameter of 23.25 mm.

exactly parallel to the reader. The used RFID temperature transponder tag TELID®211.01 is a passive sensor device with a working temperature between -40 and $140\,^{\circ}\mathrm{C}$. It has a resolution of $0.0625\,\mathrm{K}$ and an accuracy of $\pm 0.5\,\mathrm{K}$ in the range of $0\,^{\circ}\mathrm{C}$ to $65\,^{\circ}\mathrm{C}$ and $\pm 1\,\mathrm{K}$ in the range of $-40\,^{\circ}\mathrm{C}$ to $125\,^{\circ}\mathrm{C}$ [48]. The TELID has a diameter of $d_{\mathrm{TELID}} = 14\,\mathrm{mm}$ and a maximum height of $h_{\mathrm{TELID}} = 2\,\mathrm{mm}$ in an half lens housing. A photograph of the used parts is shown in Fig. 1, where the reader, antenna, tags, and the used particles are shown.

The RFID tags are delivered with calibration parameters, which are securely stored within the memory of each tag. As the system originates from a commercial manufacturer, access to the calibration data is not feasible. Nevertheless, the system was received directly from the manufacturer with a recent calibration, and it was immediately utilized for the experiments conducted. Therefore, it is reasonable to assume that the temperature measurements of the RFID tags are appropriately calibrated. The communication distance between the tags and the corresponding antenna is 20 mm. To ensure an alignment of the antenna to the tag, where the communication is stable, the reader also has a search mode in addition to the measurement mode. In this mode, only the number of tags currently found is displayed, so that stable communication between the reader and tag can be established by moving the antenna accordingly. After that, it is possible to switch the reader to the measuring mode, in which the data is recorded for a preset period of time and at certain intervals.

2.2.1. Temperature Measurement at Axial Positions

In the first experimental setup, the temperature is investigated in a fixed bed, with four tags placed in the axial direction. The reactor consists of a glass tube with an inner diameter of $D = 25.4\,\mathrm{mm}$ and a length of $L = 600\,\mathrm{mm}$ and is filled with ring shaped particles. The ceramic particles with an outer diameter $d_{\mathrm{outer}} = 10\,\mathrm{mm}$, an inner diameter $d_{\mathrm{inner}} = 6\,\mathrm{mm}$ and a height of $h_{\mathrm{p}} = 10\,\mathrm{mm}$ are filled with a single particle drop into the reactor tube. To insert the RFID tags, they are placed at specific axial positions, just like the particles. For comparison with conventional temperature measurement, the glass tube is equipped with two K-type thermocouples with typical expected bias error of 2.2 K, which are located at the axial position 1 and 4 near the corresponding tags [49]. The reactor tube as well as the thermocouples and tags in the fixed bed are shown in Fig. 2.

With a fan heater, hot air flows through the reactor and heats up the

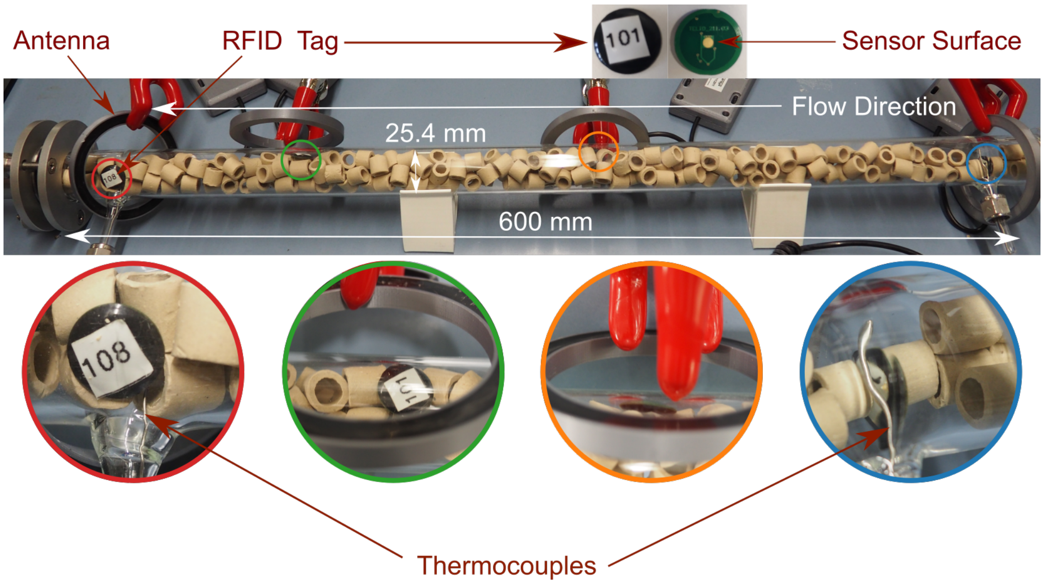

Figure 2: Experimental setup for the temperature measurement inside the fixed bed at different axial positions.

particles and the glass tube wall. The tube in this experiment is not thermally insulated in order to avoid possible interference with the signal due to additional shielding and to have an unobstructed optical access to the fixed bed. It should be mentioned that thermal insulation with metal, e.g. aluminum foil, is not meaningful, as it would lead to a Faraday cage that would no longer allow communication with the RFID tags. Therefore, thermal insulation with another material, e.g. glass yarn fabric, would be necessary.

2.2.2. Fixed Bed with Temperature Measurement Inside a Particle

In the second experimental setup, the temperature in a fixed bed is measured using an RFID tag inserted inside a 3D-printed particle. For this purpose, the reactor is mounted vertically and immersed in a cylinder filled with hot water. A statement can be made about whether the RFID tag does

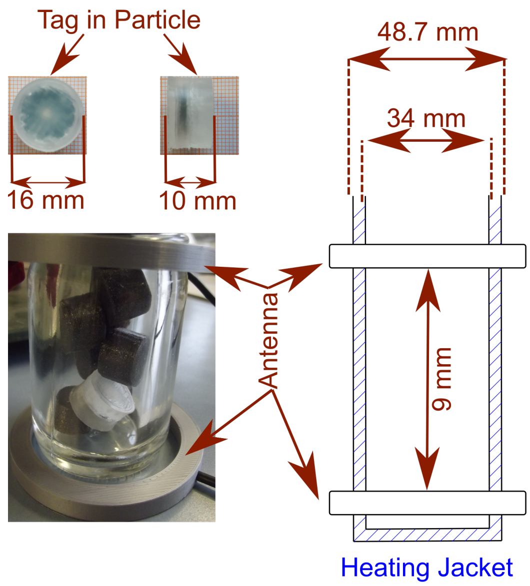

Figure 3: Experimental setup for comparison of measured fluid temperature vs. temperature inside a particle using an RFID tag in a 3D printed particle.

still operate through two layers of glass, the heating medium water, the fixed bed, and the particle itself, or whether communication is no longer possible due to the additional shielding. In addition to the temperature measurement in the particle, another RFID tag is also positioned in the packed bed. It is placed on the particle bed as in the previous experiment. Thus, the temperature of the gas phase can be compared with the temperature inside the particle. The experimental setup for this investigation is shown in Fig. 3.

Therefore, the fixed bed is filled with the particle, which has the RFID tag inside, as also 3D printed particles of the same size, shown in Fig. 3. The particles are additively manufactured with the Ultimaker 3 3D printer from Ultimaker B.V. (Urecht, the Netherlands) using polypropylene (PP) for the particle with RFID tag and polylactic acid (PLA) for the other particles.

Although the melting points of the 3D printing filaments used are higher, they are only dimensionally stable up to approx. 65 °C, which is why a water temperature of 60 °C is selected for the heating jacket. In a further experiment, non-metallic thermal insulation is placed between the antennas and the outer wall of the heating jacket.

3. Results and Discussion

3.1. Temperature Comparison

First, the temperature of the RFID measurement system is compared with that of a conventional thermocouple. For this purpose, both are placed in an empty glass cylinder (no other particles inside). The temperature of the surrounding air is measured for 5 min and then the tube is filled with hot water. Thus, the immediate temperature rise, as well as the subsequent cooling of the water for 30 min, is recorded with both measuring methods. The two temperature profiles over time are shown in Fig. 4.

While the RFID tag and the thermocouple measure the same temperature in cool air, there is a small difference of around 2 °C when the hot water is cooled. The mean absolute deviation between the thermocouple and the RFID tag is 1.73 K, while the mean relative deviation amounts to 3.65 %. Nevertheless, the course of both curves is the same. The difference can be explained by the different positions of the tag and the thermocouple in the glass tube. While the RFID tag sinks in the water and is therefore at the bottom of the container, the thermocouple is fixed in the same radial position, but at a small distance above the RFID tag. The temperature difference can therefore be explained by a higher cooling rate at the glass tube wall.

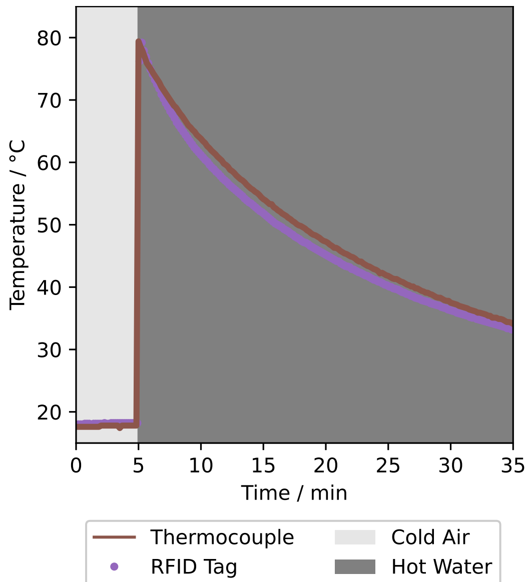

Figure 4: Temperature of an RFID tag, compared to a thermocouple in cooling water inside a cylinder.

In addition to this explanation for the temperature difference, it should be noted at this point that the observed difference is smaller than the typically expected error of a Type K thermocouple. Overall, the experiment shows that the RFID tag delivers same temperature values as a thermocouple.

3.2. Heated Fixed Bed

In the next step, the fixed bed of hollow cylinders with four tags and two thermocouples, shown in Fig. 2, is heated with a hot air stream. Firstly, constant heating is performed to obtain the temperature over time at different positions in the fixed bed. Secondly, the dynamic behavior of the temperature sensors is investigated by switching the fan heater between two temperature levels.

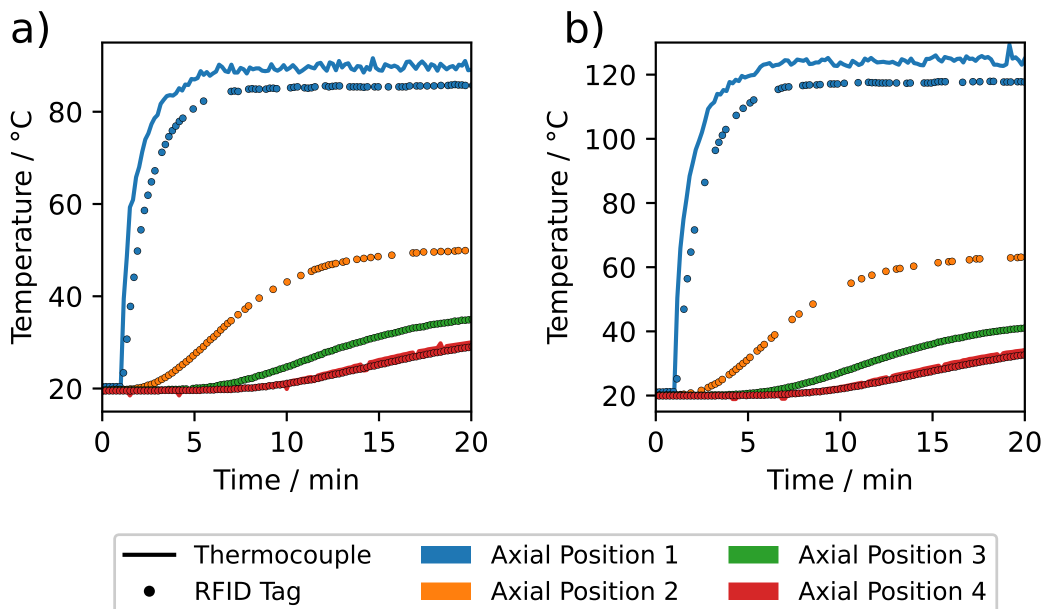

Figure 5: Temperature at different positions of a fixed bed for two different heating levels (inlet temperature: a) 100 °C, b) 130 °C) measured with RFID tags and thermocouples.

3.2.1. Constant Heating

Fig. 5 presents the temperature profiles over time for two different temperature levels and for the four axial positions in the fixed bed. Since the tube is not thermally insulated, the heat loss through the tube wall is considerable. However, the lack of insulation serves to obtain a stable signal from the tags. Shielding with metal would result in a Faraday cage, which would mean that communication between the RFID tag and the reader would no longer be possible. The particles are heated up very slowly so that the steady state is not yet reached at the rear axial positions. For axial positions 1 and 4, the temperature was also recorded with a thermocouple being place near the tags.

The variation of temperature over time shows agreement for the two temperature levels and differs only in the maximum temperature reached. It can be observed that, the foremost axial position heats up the fastest, while heating up slows down with increasing distance from the inlet. Due to the lack of heat shielding, the heat loss over the tube wall is considerable and results in only a moderate temperature rise in the axial position. While the maximum temperature for position 1 in Fig. 5 a) is approx. 85 °C, the maximum temperature for Fig. 5 b) is higher at slightly more than 120 °C. It can be observed that for both cases, the axial positions 1 and 2 have already reached a stable temperature at approx. 7 and 15 minutes, respectively, while the temperature at positions 3 and 4 are still increasing. A comparison between the thermocouples and the RFID tag shows a considerable difference only for the axial position 1. The reason for this is not a difference due to the measurement method, since both temperature sensors deliver the same values, as already shown in Fig. 4. Rather, the exact position of the sensors in the fixed bed is the source of the different temperatures. As can be seen in Fig. 2 for axial position 1 (blue encircled sub-figure down right), the RFID tag is located exactly between 2 rings. Thus, the RFID tag reports most likely the temperature of the ceramic rings rather than the temperature of the hot air stream. In contrast, the tip of the thermocouple is located in the hot air stream slightly above the rings and therefore measures the gas temperature. Unintentionally, the radial temperature profile inside the tube is reported here. In light of the variance in final temperatures observed at these two positions, it is important to note that the relatively slower heating rate exhibited by the RFID tags should not be misconstrued as indicative of a delay inherent to the measurement method. Figure 4 illustrates that both measurement methods are capable of closely replicating the same temperature profile over time when subjected to a gradual cooling process. In order to comprehensively investigate the potential presence of delay time under rapidly changing temperature conditions, further dynamic experiments will be conducted in the subsequent phase of this research.

This study shows that it is possible to record the temperature at different positions with the RFID tags inside a fixed bed and through the glass tube wall. Furthermore, it is shown that also the radial position of the temperature sensor has an influence on the measured temperature. Even though the temperature measurement with the tags in the fixed bed disturbs the structure less than with the thermocouples penetrating the fixed bed, there is still a disturbance from the RFID tags, which are shaped differently from the particles. In chapter 3.2.3, an RFID tag is therefore imprinted into a particle using additive manufacturing in order to be able to measure the temperature without affecting the structure. Of particular interest is the difference between the measured temperature in the fluid phase and in the particle itself, which will be discussed. Before that, however, the dynamic heating behavior is presented.

3.2.2. Dynamic Heating

To investigate the dynamic behavior of the temperature measurement, the system is switched between the two temperature levels. Since the thermocouple and the RFID tag measure different temperatures due to their different positions in the fixed bed, the temperature is normalized with the minimum $T_{\min}$ and the maximum temperture $T_{\max}$:

$$\Delta\theta = \frac{T - T_{\text{min}}}{T_{\text{max}} - T_{\text{min}}} \tag{1}$$

The temperature reported in the following is always that of axial position 1 from Fig. 5 (blue encircled). Fig. 6 shows the dynamic temperature $\Delta\theta$ for two different heating intervals, i.e., a) 10 min and b) 5 min. Due to the normalization of the temperature, a comparison of the dynamic behavior between the thermocouple and RFID tag is possible. For the 10 min interval, both reported temperatures show a saturation for the heating and cooling process after approx. 7 min. The temperature measured with the thermocouple exhibits fluctuations, that might originate from unsteady fluid flow conditions. Contrarily, the RFID tag shows a smooth temperature profile. Since the RFID tag is positioned between two particles, it reports the temperature of the slightly more inert solid phase. This shows that the RFID tag is also suitable for dynamic experiments in fixed bed reactors.

In Fig. 6 b) for the 5 min interval, the final temperature is not reached. This agrees with Fig. 5, where the maximum temperature at axial position 1 is not reached after 5 min. These studies show that the measurement with an RFID tag has the same quality as that with a thermocouple, since both can reproduce the same dynamic response in temperature measurement. It is worth noting that the investigations conducted provide no indication of a delay time associated with the RFID tags when compared to the thermocouples.

3.2.3. Fixed Bed with Tag in Particle

The second fixed-bed test setup compares the temperature of the fluid phase (RFID tag as-is) with the temperature measured inside a particle

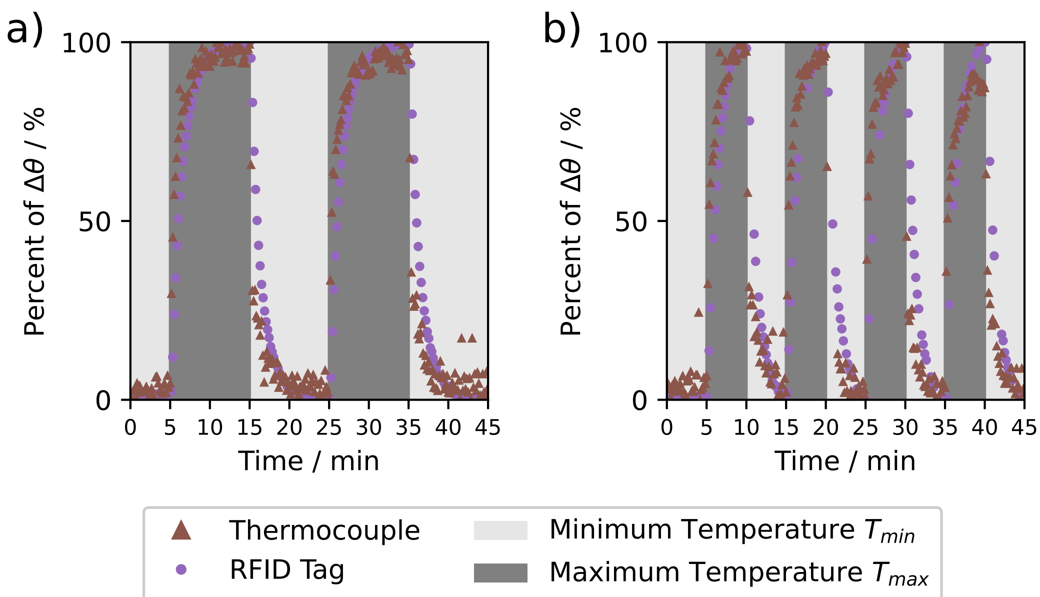

Figure 6: Dynamic behavior of the temperature for a) 10 min and b) 5 min heating/cooling intervals, normalized to the minimum and maximum temperature.

(RFID tag in the 3D-printed particle). As Fig. 7 shows, the RFID signal can pass through the two glass tube walls, the heating medium water, and the bed structure, as well as the particle itself (RFID tag in the 3D-printed particle), and thus transmits the temperature data. While the temperature is almost the same at the beginning, the RFID tag in the fluid is heated faster, while the RFID tag in the particle reaches its maximum value about 5 min later.

A difference can also be observed in the reported cooling process. Due to the delay of heating up, this starts later in the particle, whereby a lower maximum temperature is also reached. However, the particle also cools down more slowly than the fluid, which leads to an inversion in which the particle interior is warmer than the fluid starting from approx. $t = 17\,\text{min}$. This can

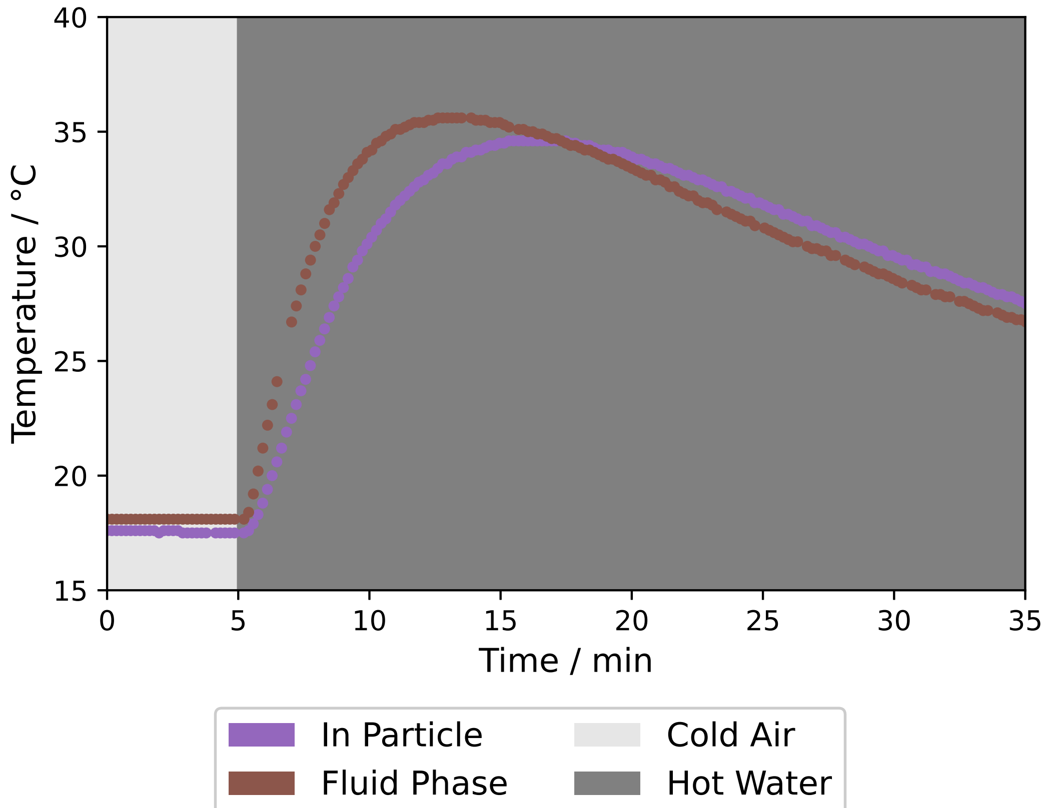

Figure 7: Comparison of the measured temperature of an RFID tag in the fluid with that of an RFID tag in a 3D-printed particle.

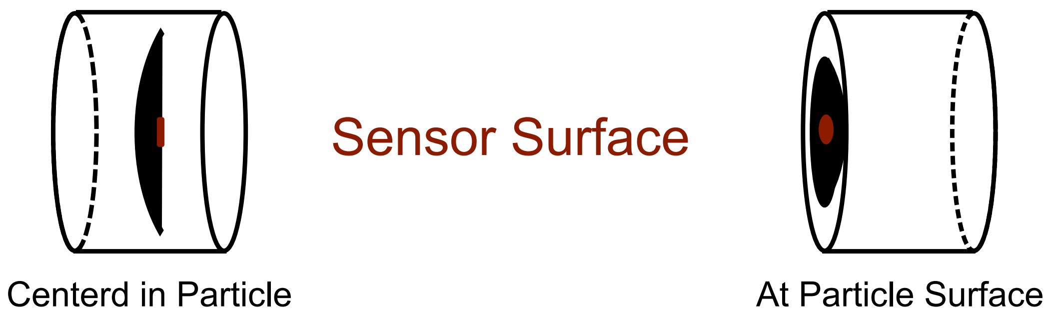

Figure 8: Possibilities of central and surface-near integration of an RFID tag inserted into a cylindrical particle.

be explained by the fact that the particle itself stores the energy through its heat capacity and thus cools down more slowly. The result shows that different temperatures are measured with the RFID tag as-is and the RFID tag in-particle when the reactor is under dynamic operation.

In the case tested here, the RFID tag is located in the center of the 3D printed particle and therefore measures the particle temperature rather than the temperature of the surrounding fluid phase. This information might be interesting for catalytic reactions, for example. For an accurate measurement of the fluid temperature without disturbing the fixed bed structure, the RFID tag could be placed in the particle so that the sensor surface is flush with the particle outer surface, see sketch in Fig. 8.

3.3. Limitations

One of the measurement system's current limitations is the gap in recorded data. While the RFID tags are found in search mode, measurement mode partially shows a data gap. Fig. 9 a) reports measurement points for all axial positions of the large fixed bed setup from Fig. 2. Especially at position 2 (orange encircled), the measurement gap is significant (less than 20% of the data is recorded). The measurement gap MG is calculated from the number of measurement points that should be made n_{set} and the actual number of received measurement points n_{obs}:

$$MG = \left(1 - \frac{n_{\mathrm{obs}}}{n_{\mathrm{set}}}\right) \cdot 100\,\% \tag{2}$$

In general, a data loss can originate from three facts. Either the electromagnetic field is not sufficient to supply the RFID tag with enough energy, or the transmission of the measured data no longer reaches the reader due to a signal strength that is too weak or by an interfering transmitter. In the presented case, the reason for the measurement gap is an unstable connection between the antenna of the reader and the RFID tag due to a non-ideal alignment of the RFID tag to the antenna. The tags have the optimal alignment when they are in the center of the antenna and oriented in line with the front face of the antenna, see Fig. 9 b). In contrast, it is not possible to receive a signal at a 90° angle to the antenna's front face. Since the orientation of the RFID tag cannot be changed exactly in a fixed bed, the antenna must be aligned accordingly, which for design reasons does not always result in an ideal antenna-tag arrangement.

In addition, care must be taken not to place the antennas too close to each other, as they also influence each other. Otherwise, it leads to a measurement gap, which becomes smaller with a larger distance between the antennas (Fig. 9 b)). The experiments are carried out with two tags with an optimal orientation to the antenna. The axial distance is varied and the measurement gap is calculated according to Eq. 2 for the corresponding an-

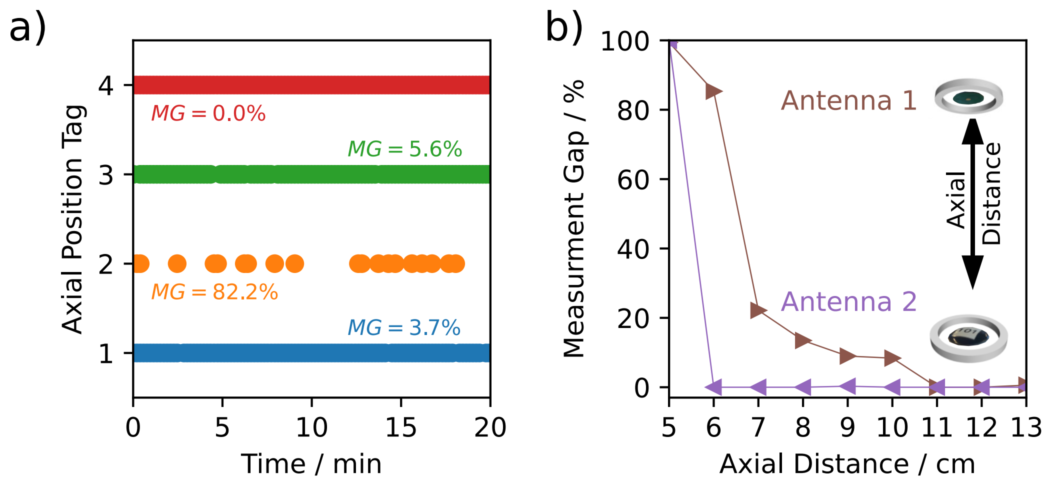

Figure 9: a) Measurement points over time for different axial positions (for setup illustrated in Fig. 2) an corresponding measurement gap; b) measurement gap as a function of the axial distance between two antennas.

tennas. At an axial distance of 5 cm both antennas receive no signal from the tags. For larger distances, almost all measurement points from antenna 2 are received. Contrarily, antenna 1 shows a large measurement gap of 80 % at 6 cm, which decreases to a value of about 10 % when the distance is increased to 10 cm. At a distance of more than 10 cm, the measurement gap drops to 0 % and there is no longer any mutual interference. Since the system under consideration operates in the HF range (13.56 Hz), it is difficult for the reader to assign the signals correctly. These results show that with the current RFID technology, a distance of 10 cm between tags must be maintained to ensure complete data collection. Compared to other axial temperature measurement setups for fixed bed reactors, this appears to be a major disadvantage in axial resolution, since FBGs, for example, can have millimeter resolution. An improvement seems to be achievable with a system that operates in a different frequency range and thus uses tags with different frequencies. Also, the current communication distance of 20 mm is still too low, as it clearly limits the fixed bed reactor outer diameter.

Furthermore, the current dimensions of the RFID tags ($d = 10\,\mathrm{mm}$) used is a major drawback. Particles with inserted RFID tags are much larger than the typical size of catalytic fixed bed reactor pellets, which are in a range between 5-10 mm in diameter and height [5]. Therefore, the RFID tags must be made smaller, which especially affects the antenna design of the tags.

In addition, the signal is shielded by metal-containing thermal insulation and above all cannot be transmitted through any kind of metal (Faraday cage). Therefore, current applications are still limited to research reactors made of glass and without metallic thermal insulation. Furthermore, without direct optical visibility, it is difficult to accurately determine the axial position of the RFID tag. This can only be realized via the signal strength to the antennas. Determining the exact radial position, on the other hand, is not yet possible according to the current state of the art. Additionally, the tags used in this work are limited to a maximum temperature of 140 °C due to their semiconductor technology. This is still too low for chemical engineering applications in reactive fixed beds and would therefore have to be significantly increased by using other materials. It is worth mentioning that there is already semiconductor technology based on the material Silicon Carbide (SiC), which can also operate in a temperature range of up to 500 °C [50].

4. Conclusions

This study shows that it is possible to accurately measure the temperature in a fixed bed reactor using current RFID technology without disturbing the bed structure (non-invasive measurement). The RFID tags can be placed directly at different positions in the fixed bed, although this slightly influence the local bed structure. If RFID tags are integrated into particles, with for example 3D printing techniques, the original bed structure can be maintained. This is especially meaningful for low tube-to-particle-diameter ratio fixed bed arrangements, where thermowells highly influence the reactor behavior [19, 20]. The advantages of such a system can be summarized as follows:

- Dynamic temperature measurement within the fixed bed.
- Minimal/No impact on the fixed bed structure; temperature measurements represent the entire tube bundle effectively.

At the moment, RFID technology can be used in lab-scale reactors to accurately measure temperature at moderate levels. In order to use RFID in industrial-relevant catalytic fixed bed reactors, further research is needed. Current limitations include:

- The current range limitation of the RFID tags is approx. 20 mm, when using the high-frequency range.
- The signal is shielded by thermal insulation, especially if it contains metal and thus forms a Faraday cage.

- Axial resolution is limited to about 10 cm due to mutual interference of neighboring antennas.

- Measurement gaps occur up to 100%, if the distance between antennas is too small.

- Measurement gaps are caused by the alignment of the particles to the antenna.

- The dimensions of the RFID tags are too large.

While the range could be improved by signal strength or change of frequency, the shielding of a Faraday cage cannot be overcome. In this case, appropriate non-metallic materials and insulation should rather be considered. The alignment in the fixed bed cannot be influenced, since the particles are randomly arranged in the reactor. This requires a suitable antenna system that can detect the signals from the RFID tags regardless of their orientation and position in the fixed bed. The size of the RFID tags must also be minimized to fit into smaller particles.

Nevertheless, it has been shown that temperature measurement with RFID technology in fixed beds is possible and relatively simple, and has some advantages over thermocouples that disturb the fixed bed structure. Furthermore, this technology allows the measurement of temperature inside a particle, which makes completely new experimental data accessible, for example for single catalytic particle studies [51, 52], and the temperature in the fixed bed can be measured completely without disturbing the structure. In addition to the measurement of temperature, there is great interest to measure contactless with RFID other quantities, such as pressure and concentration, in fixed bed reactors. Overall, it has been demonstrated that temperature monitoring in fixed bed reactors using RFID tags can offer an advantage by providing temperature profiles from tubes with a representative structure. However, further research is still required to address the challenges highlighted.

Author Contributions

Steffen Flaischlen: Conceptualization, Methodology, Validation, Formal analysis, Investigation, Writing - Original Draft, Visualization **Gregor D. Wehinger:** Conceptualization, Methodology, Writing - Review & Editing, Supervision, Project administration, Funding acquisition

Acknowledgments

This publication is based upon work supported and financed by Clausthal University of Technology, project Catalytic and microbial methanation as basis for sustainable energy storage (CliMb).

Conflicts of Interest

The authors declare no conflict of interest.

Symbols used

Latin Letters

d_{inner}	mm	Inner Ring Diameter
d_{p}	mm	Particle Diameter
d_{outer}	mm	Outer Ring Diameter
d_{TELID}	mm	RFID tag Diameter
D	mm	Reactor Diameter
h_{p}	mm	Ring Particle Height
h_{TELID}	mm	RFID tag height
L	mm	Reactor Length
MG	%	Measurement Gap
n_{obs}		Observed Number of Measurements
n_{set}		Theoretical Number of Measurements
t	min	Time
T	°C	Temperature

Greek Letters

Δ	Difference
θ	Dimensionless Temperature

Sub- and superscripts

max	Maximum
min	Minimum

Abbreviations

CFD	Computational Fluid Dynamics
DOFS	Distributed Optical Fiber Sensing
DTS	Distributed Temperature Sensing
FBG	Fiber Bragg Grating
HF	High Frequency
RFID	Radio Frequency Identification
TSP	Temperature Sensitive Paint
UHF	Ultra-High Frequency

References

[1] F. S. Mederos, J. Ancheyta, J. Chen, Review on criteria to ensure ideal behaviors in trickle-bed reactors, Applied Catalysis A: General 355 (1) (2009) 1–19. doi:10.1016/j.apcata.2008.11.018.

[2] M. Dorn, F. Eschbach, D. Hekmat, D. Weuster-Botz, Influence of different packing methods on the hydrodynamic stability of chromatography columns, Journal of Chromatography A 1516 (2017) 89–101. doi:10.1016/j.chroma.2017.08.019.

[3] A. C. Kadak, A future for nuclear energy: pebble bed reactors, International Journal of Critical Infrastructures 1 (4) (2005) 330–345. doi:10.1504/IJCIS.2005.006679.

[4] G. Eigenberger, W. Ruppel, Catalytic fixed-bed reactors, in: Ullmann's Encyclopedia of Industrial Chemistry, John Wiley & Sons, Ltd, 2012, pp. 1–66. doi:10.1002/14356007.b04_199.pub2.

[5] G. D. Wehinger, Improving the radial heat transport and heat distribution in catalytic gas-solid reactors, Chemical Engineering and Processing - Process Intensification 177 (2022) 108996. doi:10.1016/j.cep.2022.108996.

[6] N. Jurtz, G. D. Wehinger, U. Srivastava, T. Henkel, M. Kraume, Validation of pressure drop prediction and bed generation of fixed-beds with complex particle shapes using discrete element method and computational fluid dynamics, AIChE Journal 66 (6) (2020) e16967. doi:10.1002/aic.16967.

[7] G. D. Wehinger, T. Eppinger, M. Kraume, Evaluating Catalytic Fixed-Bed Reactors for Dry Reforming of Methane with Detailed CFD, Chemie Ingenieur Technik 87 (6) (2015) 734–745. doi:10.1002/cite.201400153.

[8] P. Andrigo, R. Bagatin, G. Pagani, Fixed bed reactors, Catalysis Today 52 (2) (1999) 197–221. doi:10.1016/S0920-5861(99)00076-0.

[9] A. Fache, F. Marias, V. Guerré, S. Palmade, Optimization of fixed-bed methanation reactors: Safe and efficient operation under transient and steady-state conditions, Chemical Engineering Science 192 (2018) 1124–1137. doi:10.1016/j.ces.2018.08.044.

[10] J. C. Thoméo, C. O. Rouiller, J. T. Freire, Experimental analysis of heat transfer in packed beds with air flow, Industrial & Engineering Chemistry Research 43 (2004) 4140–4148. doi:10.1021/ie030759u.

[11] D. Edouard, T. Truong Huu, C. Pham Huu, F. Luck, D. Schweich, The effective thermal properties of solid foam beds: Experimental and estimated temperature profiles, International Journal of Heat and Mass Transfer 53 (19) (2010) 3807–3816. doi:10.1016/j.ijheatmasstransfer.2010.04.033.

[12] I. Gräf, A.-K. Rühl, B. Kraushaar-Czarnetzki, Experimental study of heat transport in catalytic sponge packings by monitoring spatial temperature profiles in a cooled-wall reactor, Chemical Engineering Journal 244 (2014) 234–242. doi:10.1016/j.cej.2014.01.060.

[13] Y. Dong, B. Sosna, O. Korup, F. Rosowski, R. Horn, Investigation of radial heat transfer in a fixed-bed reactor: CFD simulations and profile measurements, Chemical Engineering Journal 317 (2017) 204–214. doi:10.1016/j.cej.2017.02.063.

[14] G. D. Wehinger, M. Kraume, V. Berg, O. Korup, K. Mette, R. Schlögl, M. Behrens, R. Horn, Investigating dry reforming of methane with spatial reactor profiles and particle-resolved CFD simulations, AIChE Journal 62 (12) (2016) 4436–4452. doi:10.1002/aic.15520.

[15] Y. Dong, M. Geske, O. Korup, N. Ellenfeld, F. Rosowski, C. Dobner, R. Horn, What happens in a catalytic fixed-bed reactor for n-butane oxidation to maleic anhydride? Insights from spatial profile measurements and particle resolved CFD simulations, Chemical Engineering Journal 350 (2018) 799–811. doi:10.1016/j.cej.2018.05.192.

[16] T. Mongkhonsi, H. F. LóApez-Isunza, L. S. Kershenbaum, The distor-

tion of measured temperature profiles in fixed-bed reactors, Chemical Engineering Research and Design 70 (3) (1992) 255–264.

[17] V. Landon, Temperature correction for packed bed multitubular reactors with concentric axial thermowells, Computers & Chemical Engineering 20 (5) (1996) 475–481. doi:10.1016/0098-1354(95)00178-6.

[18] A. G. Dixon, Y. Wu, Flow and heat transfer in narrow fixed beds with axial thermowells, Numerical Heat Transfer, Part A: Applications 76 (11) (2019) 811–829. doi:10.1080/10407782.2019.1673084.

[19] A. G. Dixon, Y. Wu, Partial oxidation of o-xylene to phthalic anhydride in a fixed bed reactor with axial thermowells, Chemical Engineering Research and Design 159 (2020) 125–137. doi:10.1016/j.cherd.2020.03.027.

[20] M. Kutscherauer, P. Reinold, S. Böcklein, G. Mestl, T. Turek, G. D. Wehinger, How temperature measurement impacts pressure drop and heat transport in slender fixed beds of raschig rings, ACS Engineering Au 3 (1) (2023) 45–58. doi:10.1021/acsengineeringau.2c00039.

[21] M. A. Mentzer, Fiber optic sensors, in: R. G. Hunsperger (Ed.), Photonic Devices and Systems, Taylor & Francis Group, 2017, pp. 1–31. doi:10.1201/9780203743515.

[22] J. Meyer, A. Nedjalkov, C. Kelb, G. J. Strobel, L. Ganzer, W. Schade, Manufacturing and characterization of femtosecond laser-inscribed bragg grating in polymer waveguide operation in an IR-A wavelength range, Sensors 20 (1) (2020). doi:10.3390/s20010249.

[23] C. Stegehake, M. Grünewald, Anwendung von faseroptischer Messtechnik zur gering-invasiven Temperaturprofilmessung in Reaktoren, Chemie Ingenieur Technik 89 (4) (2017) 480–485. doi:10.1002/cite.201600138.

[24] C. Stegehake, M. Grünewald, H.-W. Zanthoff, C. Hecht, Faseroptische Temperaturprofilmessungen in Festbettreaktoren zur modellgestützten Evaluierung der effektiven radialen Wärmeleitung, Chemie Ingenieur Technik 90 (5) (2018) 602–614. doi:10.1002/cite.201700158.

[25] C. Herrera, G. Nellis, D. Reindl, S. Klein, J. M. Tinjum, A. McDaniel, Use of a fiber optic distributed temperature sensing system for thermal response testing of ground-coupled heat exchangers, Geothermics 71 (2018) 331–338. doi:10.1016/j.geothermics.2017.10.002.

[26] Z. Ahmed, C. Jordan, P. Jain, K. Robb, H. Bindra, S. J. Eckels, Experimental investigation on the coolability of nuclear reactor debris beds using seawater, International Journal of Heat and Mass Transfer 184 (2022) 122347. doi:10.1016/j.ijheatmasstransfer.2021.122347.

[27] J. Bremer, Advanced operating strategies for non-isothermal fixed-bed reactors exemplified for CO_2 methanation, Ph.D. thesis, Magdeburg: Otto-von-Guericke-Universität (2020).

[28] R. Horn, O. Korup, M. Geske, U. Zavyalova, I. Oprea, R. Schlögl, Reactor for in situ measurements of spatially resolved kinetic data in heterogeneous catalysis, Review of Scientific Instruments 81 (6) (2010). doi:10.1063/1.3428727.

[29] T. Liu, J. P. Sullivan, K. Asai, C. Klein, Y. Egami, Pressure and temperature sensitive paints, 2nd Edition, Experimental fluid mechanics, Springer, Cham, 2021. doi:10.1007/978-3-030-68056-5.

[30] G. P. Russo, 5 - Temperature measurements, in: Aerodynamic Measurements, Woodhead Publishing, 2011, pp. 143–160. doi:10.1533/9780857093868.143.

[31] T. Liu, J. P. Sullivan, K. Asai, C. Klein, Y. Egami, Applications of TSP, in: Pressure and Temperature Sensitive Paints, Springer, Cham, 2021, pp. 345–398, series Title: Experimental Fluid Mechanics. doi:10.1007/978-3-030-68056-5_10.

[32] C. Heizer, J. Crager, Thermal Insulation Having An RFID Device, US Patent App. 14/250,283 (Oct. 16 2014).

[33] C. Heizer, L. Niblett, Heating Cable Having An RFID Device, US Patent App. 14/250,288 (Oct. 16 2014).

[34] A. J. R. Hillier, V. Makarovaite, C. W. Gourlay, S. J. Holder, J. C. Batchelor, A passive UHF RFID dielectric sensor for aqueous electrolytes, IEEE Sensors Journal 19 (14) (2019) 5389–5395. doi:10.1109/JSEN.2019.2909353.

[35] K. H. Eom, M. C. Kim, S. Lee, C. won Lee, The vegetable freshness monitoring system using RFID with oxygen and carbon dioxide sensor, International Journal of Distributed Sensor Networks 8 (6) (2012) 472986. doi:10.1155/2012/472986.

[36] C. Surman, R. A. Potyrailo, W. G. Morris, T. Wortley, M. Vincent, R. Diana, V. Pizzi, J. Carter, G. Gach, Temperature-independent passive RFID pressure sensors for single-use bioprocess components, in: 2011 IEEE International Conference on RFID, 2011, pp. 78–84. doi:10.1109/RFID.2011.5764640.

[37] K. Ong, C. Grimes, C. Robbins, R. Singh, Design and application of a wireless, passive, resonant-circuit environmental monitoring sensor, Sensors and Actuators A: Physical 93 (1) (2001) 33–43. doi:10.1016/S0924-4247(01)00624-0.

[38] A. G. Dixon, Local transport and reaction rates in a fixed bed reactor tube: Endothermic steam methane reforming, Chemical Engineering Science 168 (2017) 156–177. doi:10.1016/j.ces.2017.04.039.

[39] B. Partopour, A. G. Dixon, n-butane partial oxidation in a fixed bed: A resolved particle computational fluid dynamics simulation, The Canadian Journal of Chemical Engineering 96 (9) (2018) 1946–1956. doi:10.1002/cjce.23130.

[40] Hipolito, A.I., Rolland, M., Boyer, C., de Bellefon, C., Single pellet string reactor for intensification of catalyst testing in gas/liquid/solid configuration, Oil Gas Sci. Technol. - Rev. IFP Energies nouvelles 65 (5) (2010) 689–701. doi:10.2516/ogst/2009079.

[41] J. Fernengel, L. Bolton, O. Hinrichsen, Characterisation and design of single pellet string reactors using numerical simulation, Chemical Engi-

neering Journal 373 (2019) 1397–1408. doi:10.1016/j.cej.2019.03.114.

[42] J. Fernengel, L. Bolton, O. Hinrichsen, Numerical investigation of pressure drop in single pellet string reactors, Chemical Engineering & Technology 43 (1) (2020) 172–178. doi:10.1002/ceat.201900372.

[43] C. Roberts, Radio frequency identification (RFID), Computers & Security 25 (1) (2006) 18–26. doi:10.1016/j.cose.2005.12.003.

[44] Y. Xiao, S. Yu, K. Wu, Q. Ni, C. Janecek, J. Nordstad, Radio frequency identification: technologies, applications, and research issues, Wireless Communications and Mobile Computing 7 (4) (2007) 457–472. doi:10.1002/wcm.365.

[45] S. A. Weis, RFID (radio frequency identification): Principles and applications, System 2 (3) (2007) 1–23.

[46] K. Finkenzeller, RFID Handbook: Fundamentals and Applications in Contactless Smart Cards, Radio Frequency Identification and Near-Field Communication, John Wiley & Sons, 2010.

[47] Dutch Society for Precision Engineering (DSPE), Thermomechanics - 5.2.6 semiconductor temperature sensors (2023).
URL https://www.dspe.nl/knowledge/thermomechanics/chapter-5-measurement/5-2-contact-sensors/5-2-6-semiconductor-temperature-sensors/

[48] Micro-Sensys GmbH, Product Datasheet - TELID ® 211.01 (2023).

URL https://www.microsensys.de/produkte/rfid-sensoren/rfid-sensor-transponder/

[49] J.-C. Han, L. Wright, Experimental Methods in Heat Transfer and Fluid Mechanics, CRC Press, 2020.

[50] J. Casady, R. Johnson, Status of silicon carbide (SiC) as a wide-bandgap semiconductor for high-temperature applications: A review, Solid-State Electronics 39 (10) (1996) 1409–1422. doi:10.1016/0038-1101(96)00045-7.

[51] B. Sosna, O. Korup, R. Horn, Probing local diffusion and reaction in a porous catalyst pellet, Journal of Catalysis 381 (2020) 285–294. doi:10.1016/j.jcat.2019.11.005.

[52] G. D. Wehinger, B. Kreitz, C. F. Goldsmith, Non-idealities in lab-scale kinetic testing: A theoretical study of a modular temkin reactor, Catalysts 12 (3) (2022) 349. doi:10.3390/catal12030349.